J. Fluid Mech. (1978), *vol.* 87, *part* 3, *pp.* 497-520
Printed in Great Britain

Recycling flow over bottom topography in a rotating annulus

By M. K. DAVEY

Department of Applied Mathematics and Theoretical Physics,
University of Cambridge†

(Received 7 March 1977 and in revised form 8 November 1977)

Steady flow of an incompressible homogeneous fluid over shallow topography in a rotating annulus is considered. The flow is driven by a differentially rotating lid. The recycling nature of the system means that prescribed upstream conditions are not available to close the problem. Consideration of the balance of transport across streamlines for the geostrophic flow leads to a general circulation condition; namely $\Gamma(\psi) = \frac{1}{2}\Gamma_T(\psi)$, where ψ is the stream function for the geostrophic flow, Γ is the circulation around a streamline and Γ_T is the circulation around the same path calculated using the prescribed upper surface velocity. Using this condition, stream functions for the linear viscous and nonlinear quasi-inviscid flow can be found. Solutions for these two limits, and linearized perturbation solutions for the transition regime between them, are presented for flow over ridges in the annulus.

1. Introduction

It is well known that small variations in bottom topography in a rapidly rotating system can cause large deviations in a current passing over them. The relevance of this phenomenon to geophysical problems, such as ocean currents crossing submarine ridges, has been the motivation for several studies. For example Boyer (1971*a*, *b*) has investigated steady homogeneous flow over infinitely long, shallow ridges theoretically and experimentally, considering both viscous and inertial effects. Huppert & Stern (1974*a*, *b*) have studied homogeneous and stratified systems with side walls. They found the effect of side walls on the flow over an obstacle, and showed that in the stratified case ageostrophic effects are important near the side walls.

These and other theories rely on the specification of a known upstream flow. For some systems, however, no such upstream region can be defined. An example of such a system is the Antarctic Circumpolar Current, which is a mean eastward flow in an annular region roughly bounded by the circles of latitude at 50 °S and 65 °S. It is a deep current, and consequently its path is influenced by the bottom topography. The aim of the theory presented here is to find a way of solving the recycling problem for conditions varying from linear viscous (when advection effects are negligible) to almost inviscid (when inertial effects dominate).

With particular reference to the Antarctic Circumpolar Current, the recycling problem has been examined previously by Kamenkovich (1962) and Johnson & Hill (1975). These papers differ from the present case in that topographic variations comparable

† Present address: National Centre for Atmospheric Research, Boulder, Colorado 80303.

with the ocean depth and linear viscous flow with a varying Coriolis parameter f were considered. Under these conditions, to a first approximation, the current follows lines of constant f/H, where H is the varying ocean depth. The existence of a circumpolar current then depends upon the presence of suitable closed f/H contours. Unfortunately no such contours exist in the Antarctic region. (Contours of H/f have been given by Gill & Parker 1970.) These theories show however that the circumpolar volume transport is strongly influenced by the topography. More recently Hart (1977) has investigated rotating flow in a cylinder, with potential vorticity conserved to zeroth order, and shown how topography can influence the zonal transport.

In the theory presented in this paper, the effects of shallow obstacles are analysed and it is found that these can have a large effect on the transport. The particular system considered is a rotating annulus with homogeneous flow driven by a differentially rotating lid. Some solutions are given for plateau topography which varies azimuthally only. Laboratory experiments with qualitatively similar topography have been carried out by Maxworthy (1977), and there is qualitative agreement between his experiments and this theory.

In § 2 the general non-dimensional equations governing the zeroth-order geostrophic flow are given. The dynamics of different parameter regimes are explained and related in terms of a spin-up length. In § 3 the conditions needed to close the problem are found by considering the radial transport balance. The general result is

$$\Gamma(\psi) = \tfrac{1}{2}\Gamma_T(\psi),$$

where ψ is the stream function for the geostrophic flow, Γ is the circulation around a streamline and Γ_T is the circulation around the same path calculated with the prescribed velocity of the upper surface. For the linear viscous regime it is shown that, taken together with the obvious boundary conditions, this result is both necessary and sufficient for a unique solution. It is thought also to be necessary and sufficient in the other regimes studied.

Linearized perturbation solutions for all regimes, assuming very shallow topography, are given in § 4, and the transport is obtained correct to second order in the topography height. The relation of our solutions for the inviscid regime to those determined independently by Hart (1977) for a cylinder will be discussed in § 4. Exact solutions for linear viscous and inviscid flow are given in §§ 5 and 6. Finally the results are summarized and points of qualitative agreement with experiments are noted.

2. The basic equations and parameter regimes

A cylindrical polar co-ordinate system (r, θ, z) rotating with angular velocity $(0, 0, \Omega)$ is chosen. The components of velocity relative to the rotating frame of reference are (u, v, w). Let ρ be the density of the fluid, assumed constant, and ν the constant coefficient of kinematic viscosity. The reduced pressure p is defined by

$$p = P + \rho\phi - \tfrac{1}{2}\rho\Omega^2 R^2,$$

where P is the fluid pressure, $\nabla\phi$ represents body forces (it is assumed that only body forces which can be expressed in terms of a potential ϕ are present) and R is the horizontal distance from the axis of rotation.

Non-dimensional variables are defined as follows:

$$\mathbf{u} = U(u^*, v^*, w^* H/L), \quad r = Lr^*, \quad z = Hz^*, \quad p = 2\Omega\rho UL p^*, \tag{2.1}$$

where the non-dimensional quantities are temporarily denoted by asterisks. The characteristic scale of the horizontal velocity is U, L is a horizontal length scale and H is a vertical length scale, taken as the height of the annulus in the absence of topography.

The non-dimensional momentum and continuity equations for incompressible flow are (dropping the asterisks)

$$\epsilon(\mathbf{u}.\nabla u - v^2/r) - v = -p_r + \tfrac{1}{2}Eu_{zz} + \tfrac{1}{2}E\gamma^2(\nabla_H^2 u - 2v_\theta/r^2 - u/r^2), \tag{2.2a}$$

$$\epsilon(\mathbf{u}.\nabla v + uv/r) + u = -p_\theta/r + \tfrac{1}{2}Ev_{zz} + \tfrac{1}{2}E\gamma^2(\nabla_H^2 v + 2u_\theta/r - v/r^2), \tag{2.2b}$$

$$\gamma^2\epsilon\mathbf{u}.\nabla w = -p_z + \tfrac{1}{2}E\gamma^2(\gamma^2\nabla_H^2 w + w_{zz}), \tag{2.2c}$$

$$\nabla.\mathbf{u} = 0, \tag{2.3}$$

where ∇_H^2 is the horizontal part of the Laplacian operator. The following non-dimensional parameters appear:

$$\epsilon = U/2\Omega L \quad \text{(the Rossby number)},$$

$$E = \nu/\Omega H^2 \quad \text{(the Ekman number)}$$

and

$$\gamma = H/L \quad \text{(the aspect ratio)}.$$

Both ϵ and E are assumed small ($\epsilon, E \ll 1$) and the case $\gamma \lesssim 1$ is considered. (These magnitudes are characteristic of large-scale geophysical flows and most of their laboratory analogues.) Asymptotically, γ is taken to be at most $O(1)$ as $\epsilon, E \to 0$.

An equation for the vertical component ζ of the relative vorticity, obtained from (2.2) and (2.3), is

$$\epsilon\mathbf{u}.\nabla\zeta + \epsilon[v_z(rw)_r - u_z w_\theta]/r = w_z(1+\epsilon\zeta) + \tfrac{1}{2}E(\gamma^2\nabla_H^2\zeta + \zeta_{zz}). \tag{2.4}$$

If the $O(\epsilon)$ and $O(E)$ terms are neglected in (2.2) and (2.3) the system is geostrophic and the equations are degenerate. To resolve the degeneracy higher-order effects must be considered. Further, for this homogeneous fluid, the geostrophic flow is independent of z, so any boundary conditions applied to the geostrophic region will affect vertical columns of fluid uniformly. Under these circumstances small variations in bottom topography may have a strong effect on the main flow, as is well known.

The geometry of the system to be investigated is shown in figure 1. Vertical side walls are situated at $r = r_1$ and $r = r_2$. The bottom topography is given by $z = h(r, \theta)$. The bottom and side walls are at rest relative to the rotating frame of reference. The flow in the annulus is driven by a horizontal surface velocity $\mathbf{u}_T(r, \theta)$ prescribed at $z = 1$. Particular examples are later given for flow driven by a rigid lid rotating at a uniform dimensional rate $\Delta\Omega$ relative to the rotating frame. (Note that for ϵ to be small $\Delta\Omega/\Omega$ must be small.)

No-slip conditions are applied at the solid boundaries, and thin boundary layers form there. Near the side walls a complicated structure involving at least two length scales is present, similar to that of the vertical shear layers investigated by Stewartson (1957). There is a layer of thickness $O(E^{\frac{1}{3}})$ within which the vertical and normal velocity components are matched to the side-wall velocity. There is also an $O(E^{\frac{1}{4}})$ layer, which

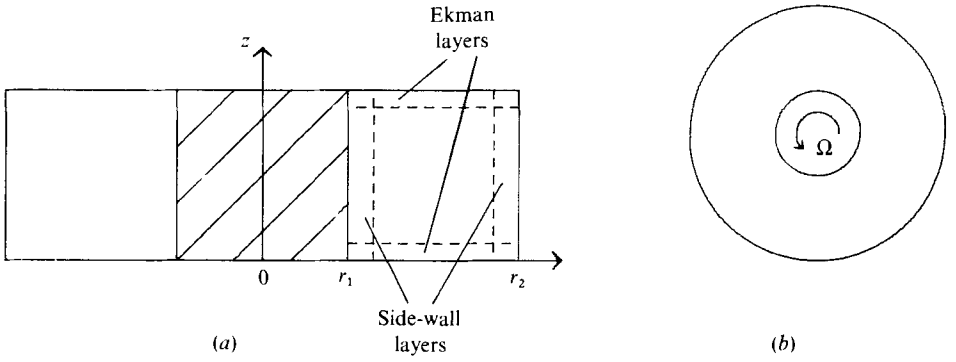

FIGURE 1. Geometry of the rotating annulus. (*a*) Cross-section through the centre, showing boundary layers. (*b*) Plan view.

is required to match the tangential component of the horizontal velocity. These side-wall layers serve only to match the $O(1)$ interior flow to the no-slip conditions on $r = r_1$ and $r = r_2$. They do not otherwise affect the dynamics of the $O(1)$ flow. The main points are that they are thin, since we assume $E^{\frac{1}{4}} \ll 1$, and that, under the terms of reference of this theory, there is no $O(1)$ geostrophic flow into these layers.

On the upper and lower boundaries there are Ekman layers of thickness $O(E^{\frac{1}{2}})$. Again, since $E^{\frac{1}{2}} \ll 1$ there is a well-defined $O(1)$ interior region, indicated by dashed lines in figure 1. The analysis of Ekman layers is a standard procedure, so only the results needed later are given here. Asymptotic expansions of the form

$$u = u^{(0)} + f(\epsilon, E)\, u^{(1)} + \ldots \tag{2.5}$$

are used. For the Ekman layers, $E^{\frac{1}{2}}$ is the appropriate form for $f(\epsilon, E)$. The analysis of the upper Ekman layer gives a boundary condition on the vertical velocity at the edge of the interior region:

$$w_I(r, \theta, 1) = \tfrac{1}{2}E^{\frac{1}{2}}(\zeta_T - \zeta_I^{(0)}) + O(E), \tag{2.6}$$

where ζ_T is the prescribed surface vorticity and the subscript I refers to the interior region. For the lower layer the variation of the bottom topography adds a kinematic term $\mathbf{u}.\nabla h$ to the Ekman suction, and the boundary condition is

$$w_I(r, \theta, h) = \tfrac{1}{2}E^{\frac{1}{2}}\zeta_I^{(0)} + \mathbf{u}_I^{(0)}.\nabla h + O(E, \epsilon h). \tag{2.7}$$

(Derivations of this condition can be found in Boyer (1971*a*) and Huppert & Stern (1974*b*).)

Equations (2.6) and (2.7) lead to restrictions on the topography which the flow can pass over and remain geostrophic. From (2.6), $w_I(r, \theta, 1)$ is $O(E^{\frac{1}{2}})$. The vorticity equation (2.4) applied to the interior says that w_{Iz} is $O(\epsilon)$ or $O(E)$, whichever is larger, and that w_{Iz} is independent of z to that order. If ϵ is $O(E^{\frac{1}{2}})$ or less, then w_I can be at most $O(E^{\frac{1}{2}})$ on the lower boundary. Hence $\mathbf{u}_I^{(0)}.\nabla h$ is restricted to $O(E^{\frac{1}{2}})$. If ϵ is greater than $O(E^{\frac{1}{2}})$, then $\mathbf{u}_I^{(0)}.\nabla h$ is similarly restricted to be $O(\epsilon)$. The result is that the geostrophic flow can pass over only topography that varies by $O(\mu)$ in the direction of flow, where

$$\mu = \max(\epsilon, E^{\frac{1}{2}}).$$

In later sections, topography consisting of ridges extending from one side wall to the other is considered. For significant flow to cross such ridges, h must be restricted to be $O(\mu)$ or less. If h is $O(1)$ as $\mu \to 0$ then the flow is blocked by the ridges, as shown by Carrier (1965). We also restrict ∇h to be $O(\mu)$, though this is not essential. (If ∇h is $O(1)$ and h is $O(\mu)$, then the flow still crosses the ridges but thin vertical ageostrophic shear layers form where ∇h is relatively large.)

The differential equation for the geostrophic flow can now be found. The vorticity equation to $O(\mu)$ contains $O(1)$ variables and the term w_{Iz}. The latter is in turn expressed in terms of $O(1)$ variables by using (2.6) and (2.7) together with

$$w_{Iz} = \mu[w_I^{(1)}(r,\theta,1) - w_I^{(1)}(r,\theta,h)] + O(E,\mu h). \tag{2.8}$$

(For interior variables, $f(\epsilon, E) = \mu$ is used in the asymptotic expansion.) Then the vorticity equation gives the approximate equation upon which the subsequent work is based:

$$\epsilon \mathbf{u}_I^{(0)} . \nabla \zeta_I^{(0)} + \mathbf{u}_I^{(0)} . \nabla h = E^{\frac{1}{2}}(\tfrac{1}{2}\zeta_T - \zeta_I^{(0)}) + O(E,\mu h). \tag{2.9}$$

The first term represents vorticity advection by the interior flow, the second term contains the topographic effect and the third term represents dissipation of vorticity by Ekman suction.

For the geostrophic interior

$$v_I^{(0)} = \partial p_I^{(0)}/\partial r, \quad u_I^{(0)} = -r^{-1}\partial p_I^{(0)}/\partial\theta.$$

Consequently a stream function can be defined by

$$\psi(r,\theta) = p_I^{(0)}(r,\theta).$$

An alternative form of (2.9) is then

$$\epsilon J(\psi, \nabla^2\psi + h/\epsilon) + E^{\frac{1}{2}}\nabla^2\psi = \tfrac{1}{2}E^{\frac{1}{2}}\zeta_T + O(E,\mu h), \tag{2.10}$$

where J is the Jacobian operator,

$$J(\psi,\chi) = r^{-1}(\psi_r\chi_\theta - \psi_\theta\chi_r).$$

Three main parameter regimes may be distinguished. If $\epsilon \ll E^{\frac{1}{2}}$, then the nonlinear inertial term is neglected in (2.9) to give

$$\zeta_I^{(0)} + \mathbf{u}_I^{(0)} . \nabla h/E^{\frac{1}{2}} = \tfrac{1}{2}\zeta_T, \tag{2.11}$$

where h is $O(E^{\frac{1}{2}})$. This is referred to as the linear viscous regime.

When $E^{\frac{1}{2}} \ll \epsilon$, the Ekman-suction term is neglected to $O(\epsilon)$ and the vorticity equation for the inviscid regime is

$$\mathbf{u}_I^{(0)} . \nabla(\zeta_I^{(0)} + h/\epsilon) = 0. \tag{2.12}$$

This means that potential vorticity $(1+\epsilon\zeta)/(1-h)$ is conserved to $O(\epsilon)$. From (2.12), $\zeta_I^{(0)} + h/\epsilon$ must be a function of the stream function alone. This gives

$$\zeta_I^{(0)} + h/\epsilon = F(\psi). \tag{2.13}$$

If the system were driven by known upstream conditions then $F(\psi)$ would be known. For the recycling problem, however, $F(\psi)$ has to be determined from the higher-order viscous effects which ultimately drive the flow.

The third regime, with $\epsilon \sim E^{\frac{1}{2}}$, is an intermediate one in which both viscous and inertial effects must be retained.

The dynamics of these regimes are linked by the concept of a spin-up length. The interior vorticity is changed by Ekman-layer dissipation on a non-dimensional time scale $E^{-\frac{1}{2}}$. A vertical column of fluid travels a distance $O(\epsilon E^{-\frac{1}{2}})$ in this time, and this distance is the spin-up length. When $\epsilon \ll E^{\frac{1}{2}}$ the spin-up length is very small, and ζ is determined locally by the topography gradient, as in (2.11). As ϵ is increased with $E^{\frac{1}{2}}$ and h unchanged (by increasing the driving rotation rate, for example), the spin-up length increases and becomes increasingly out of phase with the local topography gradient. If ϵ is increased until $\epsilon \gg E^{\frac{1}{2}}$, with h still $O(E^{\frac{1}{2}})$, then columns of fluid pass over topography variations so quickly that the Ekman suction has no time to alter the vorticity significantly. The change in ζ due to the stretching and compressing of vortex lines as h varies is $O(h/\epsilon)$, so this mechanism has a negligible effect when $h \ll \epsilon$. Hence the topography has no significant effect on the interior flow when h is much smaller than ϵ.

If h is $O(\epsilon)$ and $\epsilon \gg E^{\frac{1}{2}}$, then only the topographic stretching as a fluid column follows a streamline is important in changing the vorticity. As expressed by (2.13), this change is relative to some as yet unknown value $F(\psi)$ for each streamline.

3. Boundary and circulation conditions

To complete the formulation of the mathematical problem, boundary conditions for the differential equations are needed. Since there is no $O(1)$ flow into the side-wall layers the side walls are streamlines for the geostrophic flow, and hence $\psi(r_1, \theta)$ and $\psi(r_2, \theta)$ are both constant. These constants are related by the quantity Q defined by

$$Q = \int_{r_1}^{r_2} v_I^{(0)}\, dr = \psi(r_2, \theta) - \psi(r_1, \theta).$$

Since $\mathbf{u}_I^{(0)}$ is independent of depth and the depth is unity to zeroth order, Q is equal to the net azimuthal transport in the system to zeroth order. It is convenient to choose

$$\psi(r_1, \theta) = 0, \quad \psi(r_2, \theta) = Q. \tag{3.1a, b}$$

There is also a periodicity condition to be applied because ψ is single-valued:

$$\psi(r, \theta) = \psi(r, \theta + 2\pi). \tag{3.2}$$

The problem is not yet well posed because the constant Q cannot be determined from the differential equations and the above conditions. The extra information needed is found by considering the transport of fluid from one side wall to the other, a higher-order effect. The net transport must be zero, since the boundaries are solid and impermeable, but there are several contributing factors to be balanced against each other.

The local transport is defined by

$$\mathbf{U} = (U, V) = \int_h^1 (u, v)\, dz. \tag{3.3}$$

The $O(1)$ horizontal velocity in the Ekman layers gives an $O(E^{\frac{1}{2}})$ contribution to $\mathbf{U}$. Since the driving stress is transmitted to the interior via the Ekman layers, and it is information about the surface stress that is missing from the problem as posed so

far, the transport must be calculated to $O(E^{\frac{1}{2}})$. The local Ekman-layer transport to $O(E^{\frac{1}{2}})$ is

$$\mathbf{U}_E = E^{\frac{1}{2}}[\tfrac{1}{2}(v_T + u_T) - u_I^{(0)} - v_I^{(0)}, \tfrac{1}{2}(v_T - u_T) + u_I^{(0)} - v_I^{(0)}], \tag{3.4}$$

where (u_T, v_T) is the prescribed surface velocity.

First the linear viscous and intermediate regimes are treated together, since the Ekman layers give a first-order contribution in each case. The inviscid case is discussed later. To $O(E^{\frac{1}{2}})$,

$$\mathbf{U} = \int_h^1 (u^{(0)}, v^{(0)})\, dz + \mu \int_0^1 (u^{(1)}, v^{(1)})\, dz + \mathbf{U}_E, \tag{3.5}$$

where h is $O(\mu)$. The velocities are henceforth interior velocities, unless otherwise indicated. Consider the net transport T across a vertical sheet defined by $h \leqslant z \leqslant 1$ and any closed curve in the r, θ plane with $r_1 < r < r_2$. The transport due to $u^{(0)}$ is

$$T_0 = \oint (1-h)\, \mathbf{k} . \mathbf{u}^{(0)} \times \mathbf{dl}, \tag{3.6}$$

where the integral is taken around the closed curve with line elements $\mathbf{dl}$, and $\mathbf{k}$ is the unit vector $(0, 0, 1)$. This gives

$$T_0 = \oint h \frac{d\psi}{ds}\, ds, \tag{3.7}$$

where ds is the arc length measured along the curve. To find the first-order interior transport, the momentum equations (2.2) are used to express $(u^{(1)}, v^{(1)})$ in terms of $(u^{(0)}, v^{(0)})$. We have

$$\epsilon(\mathbf{u}^{(0)} . \nabla)\, u^{(0)} - \epsilon v^{(0)2}/r - \mu v^{(1)} = -\mu p_r^{(1)}, \tag{3.8a}$$

$$\epsilon(\mathbf{u}^{(0)} . \nabla)\, v^{(0)} + \epsilon u^{(0)} v^{(0)}/r + \mu u^{(1)} = -\mu p_r^{(1)}/r, \tag{3.8b}$$

$$p_z^{(1)} = 0. \tag{3.8c}$$

From (3.8c), $(u^{(1)}, v^{(1)})$ is independent of z. The transport due to $(u^{(1)}, v^{(1)})$ is, neglecting higher-order terms,

$$\begin{aligned} T_1 &= \mu \oint \mathbf{k} . \mathbf{u}^{(1)} \times \mathbf{dl} \\ &= -\oint \frac{d}{ds}[\mu p^{(1)} + \tfrac{1}{2}\epsilon(u^{(0)2} + v^{(0)2})]\, ds + \epsilon \oint \zeta^{(0)} \frac{d\psi}{ds}\, ds \\ &= \epsilon \oint \zeta^{(0)} \frac{d\psi}{ds}\, ds. \end{aligned} \tag{3.9}$$

The Ekman-layer transport is, from (3.4),

$$T_E = -E^{\frac{1}{2}} \oint \mathbf{u}^{(0)} . \mathbf{dl} + \tfrac{1}{2} E^{\frac{1}{2}} \oint \mathbf{u}_T . \mathbf{dl} = -E^{\frac{1}{2}}(\Gamma - \tfrac{1}{2}\Gamma_T), \tag{3.10}$$

where Γ and Γ_T denote the circulation around the curve due to the geostrophic and upper-surface velocities respectively. Note that the transport due to the upper Ekman layer is $\frac{1}{2}E^{\frac{1}{2}}(\Gamma_T - \Gamma)$ while the contribution from the lower Ekman layer is $-\frac{1}{2}E^{\frac{1}{2}}\Gamma$.

To $O(\mu)$, the net transport is

$$T = T_0 + T_1 + T_E = 0,$$

which implies that

$$\oint (\epsilon\zeta^{(0)}+h)\frac{d\psi}{ds}\,ds = E^{\frac{1}{2}}(\Gamma-\tfrac{1}{2}\Gamma_T). \tag{3.11}$$

If the path of integration is a streamline then ψ is constant, and (3.11) gives the circulation condition

$$\Gamma(\psi) = \tfrac{1}{2}\Gamma_T(\psi). \tag{3.12}$$

For a streamline that does not encircle the inner side wall (i.e. a reducible streamline), (3.12) can be derived from (2.9). The flow along such streamlines does not contribute to Q, however, so the transport analysis is necessary to close the problem.

An expression for Q can be found from (3.11) by using circles $r = r_0$ as paths of integration. This gives

$$-\int_{-\pi}^{\pi}(\epsilon\zeta^{(0)}+h)\,u^{(0)}d\theta = E^{\frac{1}{2}}\int_{-\pi}^{\pi}(v^{(0)}-\tfrac{1}{2}v_T)\,d\theta.$$

This is true for all r_0. Integrating with respect to r leads to

$$Q = Q_0-\frac{1}{2\pi E^{\frac{1}{2}}}\int_{r_1}^{r_2}\int_{-\pi}^{\pi}(\epsilon\zeta^{(0)}+h)\,u^{(0)}d\theta\,dr, \tag{3.13}$$

where

$$Q_0 = \frac{1}{2}\int_{r_1}^{r_2} v_T\,dr.$$

In the linear viscous case, the nonlinear part of (3.13) is neglected to give, after integrating by parts with respect to θ,

$$Q = Q_0-\frac{1}{2\pi E^{\frac{1}{2}}}\int_{r_1}^{r_2}\frac{1}{r}\int_{-\pi}^{\pi}h_\theta\psi\,d\theta\,dr. \tag{3.14}$$

(Here Q_0 is the net azimuthal transport when the topography is flat.) It is shown in appendix A that this condition is both necessary and sufficient for the determination of a unique stream function.

For the inviscid regime, suppose that $E^{\frac{1}{2}}$ is at least $O(\epsilon^2)$. Then the local transport to $O(E^{\frac{1}{2}})$ is, with expansions of the form $\mathbf{u} = \mathbf{u}^{(0)}+\epsilon\mathbf{u}^{(1)}+E^{\frac{1}{2}}\mathbf{u}^{(2)}+\ldots$ and

$$h = h^{(0)}+\epsilon h^{(1)}+\ldots$$

(where $h^{(i)}$ is $O(\epsilon)$),

$$\mathbf{U} = \int_h^1 (u^{(0)}, v^{(0)})\,dz+\epsilon\int_{h^{(0)}}^1 (u^{(1)}, v^{(1)})\,dz+E^{\frac{1}{2}}\int_0^1 (u^{(2)}, v^{(2)})\,dz+\mathbf{U}_E.$$

The momentum equations to $O(E^{\frac{1}{2}})$ are needed. These are

$$\epsilon^2(\mathbf{u}^{(0)}.\nabla)\,u^{(1)}+\epsilon^2(\mathbf{u}^{(1)}.\nabla)\,u^{(0)}-2\epsilon^2v^{(0)}v^{(1)}/r-E^{\frac{1}{2}}v^{(2)} = -E^{\frac{1}{2}}p_r^{(2)}, \tag{3.15a}$$

$$\epsilon^2(\mathbf{u}^{(0)}.\nabla)\,v^{(1)}+\epsilon^2(\mathbf{u}^{(1)}.\nabla)\,v^{(0)}+\epsilon^2(u^{(0)}v^{(1)}+u^{(1)}v^{(0)})/r+E^{\frac{1}{2}}u^{(2)} = -E^{\frac{1}{2}}p_\theta^{(2)}/r, \tag{3.15b}$$

$$\epsilon^2\gamma^2\mathbf{u}^{(0)}.\nabla w^{(1)} = -E^{\frac{1}{2}}p_z^{(2)}. \tag{3.15c}$$

If γ^2 is $O(1)$, then $p_z^{(2)}$ depends linearly on z because $w^{(1)}$ is linear with respect to z.

The transport across a vertical sheet is calculated as before. The second-order interior flow leads to the term

$$T_2 = E^{\frac{1}{2}} \int_0^1 \oint \mathbf{k}.\mathbf{u}^{(2)} \times \mathbf{dl}\, dz \tag{3.16a}$$

$$= -E^{\frac{1}{2}} \int_0^1 \oint \frac{dp^{(2)}}{ds} ds\, dz + \epsilon^2 \oint \zeta^{(1)} \frac{d\psi}{ds} ds - \epsilon^2 \oint \frac{d}{ds}(u^{(0)}u^{(1)} + v^{(0)}v^{(1)})\, ds - \epsilon^2 \oint \zeta^{(0)} \mathbf{k}.\mathbf{u}^{(1)} \times \mathbf{dl} \tag{3.16b}$$

$$= \epsilon^2 \oint \zeta^{(1)} \frac{d\psi}{ds} ds - \epsilon^2 \oint \zeta^{(0)} \mathbf{k}.\mathbf{u}^{(1)} \times \mathbf{dl}. \tag{3.16c}$$

The other terms in the net transport are found in the same way as in the previous case. The result is

$$T = -E^{\frac{1}{2}}(\Gamma - \tfrac{1}{2}\Gamma_T) - \epsilon \oint (h^{(0)} + \epsilon h^{(1)})\, \mathbf{k}.\mathbf{u}^{(1)} \times \mathbf{dl} + \oint (\epsilon\zeta^{(0)} + h^{(0)} + \epsilon h^{(1)}) \frac{d\psi}{ds} ds + \dot{T}_2 = 0. \tag{3.17}$$

To $O(\epsilon)$, this gives

$$\epsilon \oint F(\psi) \frac{d\psi}{ds} ds = 0.$$

No new information is gained because F and ψ are single-valued.

To $O(E^{\frac{1}{2}})$, retaining terms $O(\epsilon^2)$,

$$-E^{\frac{1}{2}}(\Gamma - \tfrac{1}{2}\Gamma_T) + \epsilon^2 \oint (\zeta^{(1)} + h^{(1)}/\epsilon) \frac{d\psi}{ds} ds + \epsilon^2 \oint F(\psi)\, \mathbf{k}.\mathbf{u}^{(1)} \times \mathbf{dl} = 0. \tag{3.18}$$

Suppose that the path of integration is a streamline. Then F is a constant and

$$\oint F(\psi)\, \mathbf{k}.\mathbf{u}^{(1)} \times \mathbf{dl} = F(\psi) \oint \zeta^{(0)} \frac{d\psi}{ds} ds.$$

Hence, with F constant, (3.18) gives

$$\Gamma(\psi) = \tfrac{1}{2}\Gamma_T(\psi). \tag{3.19}$$

This result is the same as that for the other regimes. It is a consequence of there being no net interior flow to $O(E^{\frac{1}{2}})$ across a streamline for the geostrophic flow. The flow around each streamline is in local balance with the driving stress from the surface and the dissipation at the lower boundary. The net transports across the streamline due to the upper and lower Ekman layers are equal and opposite.

Note that the circulation condition is independent of viscosity, though it is determined by viscous effects. In this respect it is analogous to the integral condition used by Batchelor (1956) for inviscid flows with closed streamlines. We have shown that the circulation condition holds for $E^{\frac{1}{2}} \sim \epsilon^n$ with $n = 1, 2$, and we conjecture that it is true for any positive integer n. For the special case ζ_T = constant (e.g. flow driven by a rigid lid), the condition can be used to prove that $Q \leqslant Q_0$ with equality if and only if $h = h(r)$. (See appendix B.)

An equation for Q for this inviscid case can be found as for the other regimes, giving

$$Q = Q_0 - \frac{\epsilon^2}{2\pi E^{\frac{1}{2}}} \int_{r_1}^{r_2} \int_{-\pi}^{\pi} (\zeta^{(0)} + h^{(0)}/\epsilon)\, u^{(1)} + (\zeta^{(1)} + h^{(1)}/\epsilon)\, u^{(0)} d\theta\, dr. \tag{3.20}$$

The vorticity equation to $O(E^{\frac{1}{2}})$ is

$$\epsilon \mathbf{u}^{(0)}.\nabla\zeta^{(0)} + \epsilon^2(\mathbf{u}^{(1)}.\nabla\zeta^{(0)} + \mathbf{u}^{(0)}.\nabla\zeta^{(1)}) = \epsilon(1 + \epsilon\zeta^{(0)})\, w_z^{(1)} + E^{\frac{1}{2}} w_z^{(2)}. \tag{3.21}$$

Using $$w_z = [E^{\frac{1}{2}}(\tfrac{1}{2}\zeta_T - \zeta) - \mathbf{u}.\nabla h]/(1-h),$$

the $O(E^{\frac{1}{2}}, \epsilon^2)$ terms in (3.21) give

$$\epsilon^2\mathbf{u}^{(1)}.\nabla(\zeta^{(0)}+h^{(0)}/\epsilon)+\epsilon^2\mathbf{u}^{(0)}.\nabla(\zeta^{(1)}+h^{(1)}/\epsilon)+\epsilon(\zeta^{(0)}+h^{(0)}/\epsilon)\,\mathbf{u}^{(0)}.\nabla h^{(0)} = E^{\frac{1}{2}}(\tfrac{1}{2}\zeta_T-\zeta^{(0)}). \tag{3.22}$$

This can be rearranged using the continuity equation to obtain

$$\epsilon^2\nabla_H.[(\zeta^{(1)}+h^{(1)}/\epsilon)\,u^{(0)}+(\zeta^{(0)}+h^{(0)}/\epsilon)\,u^{(1)}] = E^{\frac{1}{2}}(\tfrac{1}{2}\zeta_T-\zeta^{(0)}), \tag{3.23}$$

where ∇_H is the horizontal component of the gradient operator. From (3.20) and (3.23),

$$Q = Q_0 - \frac{1}{2\pi}\int_{r_1}^{r_2}\frac{1}{r}\,\lambda\int_{-\pi}^{\pi}(\tfrac{1}{2}\zeta_T-\zeta^{(0)})\,d\theta\,d\lambda\,dr. \tag{3.24}$$

[This equation also holds for the other regimes, from (2.9) and (3.13).] Hence the transport equation is independent of $E^{\frac{1}{2}}$ for the inviscid regime. This is consistent with being able to find the zeroth-order flow from (2.12) and (3.19), as in § 6.

4. Perturbation solutions

The combination of nonlinear effects and non-conservation of potential vorticity makes it very difficult to obtain general solutions of the vorticity equation (2.10) subject to the circulation condition (3.12) and the boundary conditions (3.1). However analytic approximations can be found when the disturbance to the flow is small. In this section such solutions are given for flow driven by a rigid lid. A symmetric bottom topography $h(\theta)$ represented by the Fourier series

$$h = h_0\sum_{n=0}^{\infty} g_n\cos n\theta \tag{4.1}$$

is chosen, where h_0 is a height scale.

When the topography is flat, the stream function is

$$\psi = \psi_0 = \tfrac{1}{4}\Omega_T(r^2-r_1^2), \tag{4.2}$$

where Ω_T is a non-dimensional differential rotation rate of the rigid lid. (For all examples given later, $\Omega_T = 1$ is used.) Substituting $\psi = \psi_0+\phi$ into (2.10) gives

$$\Omega_I(\epsilon\nabla^2\phi+h)_\theta + J(\phi, \epsilon\nabla^2\phi+h)+E^{\frac{1}{2}}\nabla^2\phi = 0, \tag{4.3}$$

where $\Omega_I = \frac{1}{2}\Omega_T$. To find perturbation solutions, ϕ is expanded as

$$\phi = \delta\phi_1+\delta^2\phi_2+\ldots, \tag{4.4}$$

where the expansion parameter δ is given by

$$\delta = h_0/(E+\epsilon^2\Omega_I^2)^{\frac{1}{2}}. \tag{4.5}$$

This choice of δ leads to an expansion valid for all sufficiently small ϵ and $E^{\frac{1}{2}}$.

Neglecting terms $O(\delta^2)$ as $\delta\to 0$ asymptotically in (4.3) gives

$$\delta\epsilon\Omega_I\nabla^2\phi_{1\theta}+\delta E^{\frac{1}{2}}\nabla^2\phi_1 = \Omega_I h_0\sum_{n=1}^{\infty} n g_n\sin n\theta. \tag{4.6}$$

Equation (4.6) can be solved to find the perturbation vorticity

$$\nabla^2\phi_1 = \sum_{n=1}^{\infty} A_n \cos n\theta + B_n \sin n\theta, \tag{4.7}$$

with

$$A_n = -\frac{n^2\epsilon\Omega_I^2 g_n (E+\epsilon^2\Omega_I^2)^{\frac{1}{2}}}{E+n^2\epsilon^2\Omega_I^2}, \tag{4.8a}$$

$$B_n = \frac{nE^{\frac{1}{2}}\Omega_I g_n (E+\epsilon^2\Omega_I^2)^{\frac{1}{2}}}{E+n^2\epsilon^2\Omega_I^2}. \tag{4.8b}$$

Note that $\nabla^2\phi_1$ is a function of θ only, and that it is independent of the average topography height

$$\bar{h} = (2\pi)^{-1}\int_{-\pi}^{\pi} h\, d\theta.$$

The boundary conditions needed to determine ϕ_1 are obtained from the transport equation (3.13). Using (4.3), this can be rewritten as (with an integration by parts)

$$Q = Q_0 + (2\pi E^{\frac{1}{2}}\Omega_I)^{-1}\int_{r_1}^{r_2} r^{-1}\int_{-\pi}^{\pi} \phi[J(\phi, \epsilon\nabla^2\phi + h) + E^{\frac{1}{2}}\nabla^2\phi]\, d\theta\, dr \tag{4.9a}$$

$$= Q_0 + (2\pi\Omega_I)^{-1}\delta^2\int_{r_1}^{r_2} r^{-1}\int_{-\pi}^{\pi} \phi_1\nabla^2\phi_1\, d\theta\, dr + O(\delta^3)$$

$$= Q_0 + \delta^2 Q_2 + O(\delta^3). \tag{4.9b}$$

There is no correction to Q_0 to $O(\delta)$, so the required boundary condition is

$$\phi_1 = 0 \quad \text{on} \quad r = r_1, r_2. \tag{4.10}$$

Equation (4.7) then leads to

$$\phi_1 = \sum_{n=1}^{\infty} R_n(r)[A_n \cos n\theta + B_n \sin n\theta], \tag{4.11}$$

where $R_n(r)$ is defined by

$$\left.\begin{aligned} r\frac{d}{dr}\left(r\frac{dR_n}{dr}\right) - n^2 R_n &= r^2, \\ R_n &= 0 \quad \text{on} \quad r = r_1, r_2. \end{aligned}\right\} \tag{4.12}$$

The coefficients A_n and/or B_n are $O(1)$ for all $E^{\frac{1}{2}}$ and ϵ, so ϕ_1 will be $O(1)$ and ϕ will be $O(\delta)$ as $\delta \to 0$ under all conditions. From (4.9), the correction $\delta^2 Q_2$ to the transport is

$$\delta^2 Q_2 = \delta^2(2\Omega_I)^{-1}\sum_{n=1}^{\infty}(A_n^2 + B_n^2)\int_{r_1}^{r_2} R_n r^{-1}\, dr$$

$$= \tfrac{1}{2}\Omega_I h_0^2 \sum_{n=1}^{\infty} n^2 g_n^2 (E+n^2\epsilon^2\Omega_I^2)^{-1}\int_{r_1}^{r_2} R_n r^{-1}\, dr. \tag{4.13}$$

Q_2 is $O(1)$ and, since it can be shown that R_n is negative for $r_1 < r < r_2$, the correction is always negative.

The boundary conditions for ϕ_2 are

$$\phi_2(r_1, \theta) = 0, \quad \phi_2(r_2, \theta) = Q_2. \tag{4.14}$$

Hence ϕ_2 can be calculated, and the transport determined to $O(\delta^3)$. In this manner, the solution ϕ can be found to any order in δ.

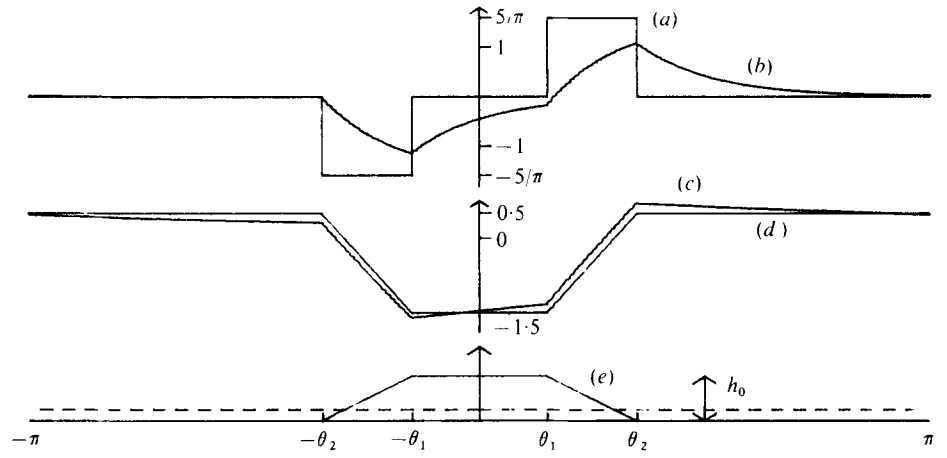

FIGURE 2. Perturbation vorticity $\delta\nabla^2\phi_1$ over plateau $h(\theta)$ with $h_0 = 0{\cdot}2$. (*a*) $E^{\frac{1}{2}} = 0{\cdot}1$, $\epsilon \to 0$. (*b*) $E^{\frac{1}{2}} = 0{\cdot}1$, $\epsilon = 0{\cdot}1$. (*c*) $E^{\frac{1}{2}} = 0{\cdot}01$, $\epsilon = 0{\cdot}1$. (*d*) $E^{\frac{1}{2}} \to 0$, $\epsilon = 0{\cdot}1$. (*e*) Plateau-topography profile $h(\theta)$.

The change in Q is caused by the nonlinear interaction of the perturbation velocity and potential vorticity. This leads to a change in the mean (zonally averaged) flow. To $O(\delta^2)$ this change is given by

$$\Phi_2(r) = (2\pi)^{-1}\int_{-\pi}^{\pi}\phi_2 d\theta = (2\Omega_I)^{-1}\sum_{n=1}^{\infty}(A_n^2+B_n^2)\int_{r_1}^{r}R_n r^{-1}dr. \tag{4.15}$$

This analysis is valid for all ϵ and $E^{\frac{1}{2}}$. In particular, solutions for the linear viscous and inviscid limits are obtained by finding the general solution and then using $\epsilon \to 0$ and $E^{\frac{1}{2}} \to 0$ respectively. The dependence on the height scale h_0 is the same in all cases. From the first approximation, the perturbation velocities depend linearly on h_0 and the transport decrease depends on h_0^2.

The perturbation vorticity $\delta\nabla^2\phi_1$ for flow over plateau topography for varying ϵ and $E^{\frac{1}{2}}$ is shown in figure 2. (The plateau for these and all subsequent examples has $\theta_1 = \frac{3}{20}\pi$ and $\theta_2 = \frac{7}{20}\pi$ and we take $r_1 = 1$ and $r_2 = 3$.) The corresponding streamlines (contours of $\psi_0 + \delta\phi_1$) are given in figure 3, and the transports $Q_0 + \delta^2 Q_2$ are given in table 1. Values of δ somewhat greater than 1 can be used, even though the theory is an asymptotic one for $\delta \to 0$. It is shown later that solutions with large δ can be good approximations to the exact solutions. One reason for this is that the large flow perturbations (e.g. flow reversal) that occur for such values of δ are restricted to small regions. Throughout most of the flow, it is found that the higher-order terms are numerically small.

For linear viscous flow, the coefficient A_n is zero and the stream function is antisymmetric with respect to θ. The perturbation vorticity is instantly dissipated in flat regions (see figure 2*a*) and is elsewhere proportional to the topography slope. The effect of recycling on the flow pattern (figure 3*a*) is small because the flow is nearly undisturbed away from the obstacle. The streamline deviation is inward over a positive slope and outward over a negative slope. When $\delta = h_0/E^{\frac{1}{2}}$ is larger than a critical value $\delta_1 = 0{\cdot}85$, a gyre appears near the inner side wall over the downstream end of the plateau. Flow reversal first occurs at $r = r_1$, $\theta \approx \frac{1}{4}\pi$. For $\delta > \delta_2 = 2{\cdot}9$ a

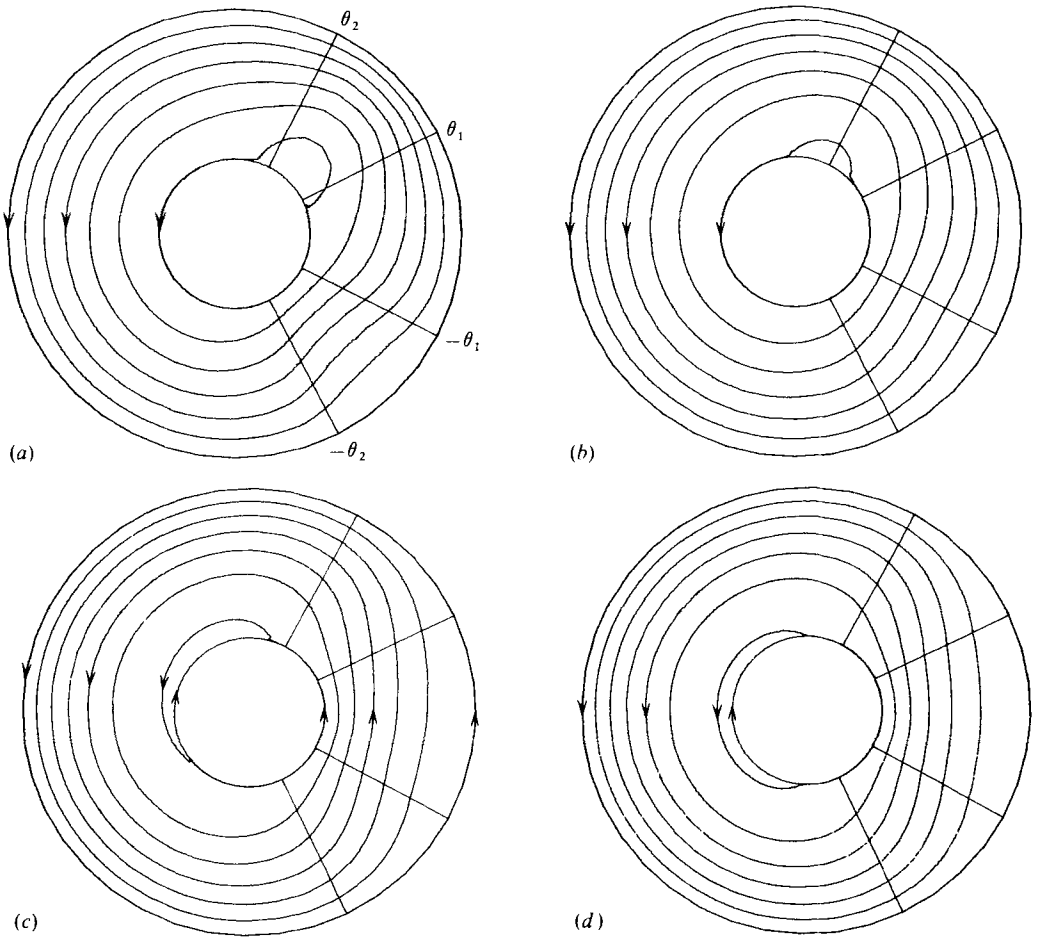

FIGURE 3. Flow over plateau topography with $h_0 = 0{\cdot}2$. The stream function $\psi_0 + \delta\phi_1$ is contoured at equal intervals. (*a*) $E^{\frac{1}{2}} = 0{\cdot}1$, $\epsilon \to 0$. (*b*) $E^{\frac{1}{2}} = 0{\cdot}1$, $\epsilon = 0{\cdot}1$. (*c*) $E^{\frac{1}{2}} = 0{\cdot}01$, $\epsilon = 0{\cdot}1$. (*d*) $E^{\frac{1}{2}} \to 0$, $\epsilon = 0{\cdot}1$.

Example	$E^{\frac{1}{2}}$	ϵ	h_0	Ω_T	Q
(*a*)	0·1	0	0·2	1	1·80
(*b*)	0·1	0·1	0·2	1	1·89
(*c*)	0·01	0·1	0·2	1	1·65
(*d*)	0	0·1	0·2	1	1·63

TABLE 1. Transport $Q = Q_0 + \delta^2 Q_2$ for the flows shown in figures 2 and 3.

second gyre appears near the inner side wall over the downstream end of the plateau. Flow reversal first occurs at the inner side wall because the undisturbed flow is slowest there. (Note that the critical δ values depend upon the shape of the obstacle. For example, $\delta_1 = 0{\cdot}86$ and $\delta_2 = 3{\cdot}6$ when $h = h_0 \cos\theta$.) Exact solutions given in the next section show that the inner gyre is a real feature and not just an artifact of the perturbation method.

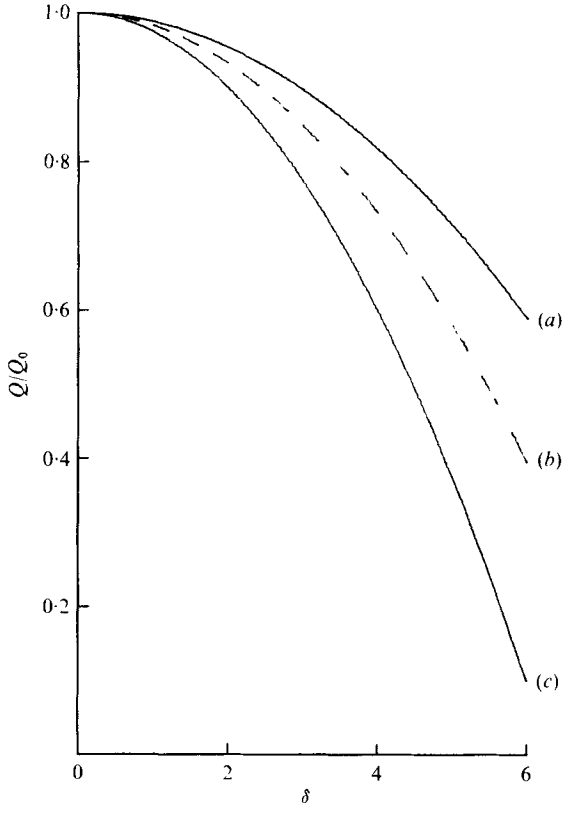

FIGURE 4. Perturbation transport $Q = Q_0 + \delta^2 Q_2$. (*a*) Inviscid limit. (*b*) Intermediate system with $\epsilon = E^{\frac{1}{2}}$. (*c*) Linear viscous limit.

The result of increasing inertial effects by increasing ϵ with fixed $E^{\frac{1}{2}}$ can be seen by comparing case (*a*) with case (*b*), which has $E^{\frac{1}{2}} = \epsilon = 0{\cdot}1$. The perturbation vorticity is advected away from the plateau and decays downstream. The gyre is shifted downstream and reduced in size. The transport change is almost halved, owing to the smoothing out of topographic effects as ϵ is increased. In going from case (*b*) to case (*c*), $E^{\frac{1}{2}}$ is reduced to 0·01 while ϵ is unchanged. Perturbation vorticity is now swept right around the annulus. Recycling affects the flow pattern over the plateau, which is almost symmetric. The transport is decreased by the dissipation decrease because the topographically generated vorticity is not being dissipated as rapidly as before. In the limit $E^{\frac{1}{2}} \to 0$ (case *d*), the coefficient B_n is zero and the flow is symmetric. The vorticity perturbation is caused by topographic stretching only. The reference level for the potential vorticity to $O(\delta)$, determined by viscous effects, is $\Omega_T + \bar{h}/\epsilon$. Hence $\nabla^2\phi_1$ is negative over the plateau, where $h > \bar{h}$, and positive away from the obstacle, where $h < \bar{h}$. As $\delta = h_0/\epsilon\Omega_I$ increases, flow reversal first occurs at the inner side wall at $\theta = \pi$ for $\delta = 3{\cdot}0$. A second gyre, centred about $\theta = 0$, forms at the outer side wall for $\delta > 4{\cdot}9$.

Hart (1977) has investigated quasi-inviscid flow in a rotating cylinder with bottom topography and a differentially rotating rigid lid. He used $\alpha = h_0/\epsilon$ as an expansion parameter and solved the problem by considering higher-order terms in the vorticity

equation with $E^{\frac{1}{2}}/\epsilon \sim \alpha$. [With α small, the vorticity equation to zeroth order is the inviscid equation (2.12).] He found that the zonal correction was $O(\alpha^2)$, and indepdent of $E^{\frac{1}{2}}$ to that order. By setting $E^{\frac{1}{2}}/\epsilon \sim \delta^n \ll 1$ in the perturbation solution given here, it is found that the flow corrections ϕ_1 and Φ_2 are given by the results in the inviscid limit. In agreement with Hart, ϕ_1 and Φ_2 are independent of $E^{\frac{1}{2}}$ and the zonal-flow correction is $O(\delta^2)$. (In fact the quasi-inviscid solution for ϕ to $O(\delta^2)$ can be obtained from the general solutions for ϕ_1 and Φ_2.) From the general solution, we further find that the zonal-flow correction is $O(\delta^2)$ for all ϵ and $E^{\frac{1}{2}}$.

The transport $Q_0 + \delta^2 Q_2$ for flow over the plateau, with $\Omega_T = 1$, is plotted against the parameter δ in figure 4. All the graphs lie between those for the inviscid and viscous limits. It can in fact be shown from (4.13) that these limits always give bounds on the general solution, within the perturbation theory.

That is, given h_0, ϵ and $E^{\frac{1}{2}}$ (and hence δ for $\Omega_T = 1$), the corresponding Q satisfies

$$Q_{\text{vis}} \leqslant Q \leqslant Q_{\text{in}} \tag{4.16}$$

correct to $O(\delta^2)$, where Q_{vis} and Q_{in} are the viscous and inviscid transports for that value of δ. Inequality (4.16) holds for any r-independent topography $h(\theta)$, but the transport curves depend on the actual shape. For instance, when $h = h_0 \cos\theta$ the Q_{vis} and Q_{in} curves (and hence all intermediate ones) are identical.

These perturbation results are good approximations when δ is sufficiently small. In the next two sections, exact solutions are found for the two limiting regimes; the term 'sufficiently small' can then be defined more precisely.

5. The linear viscous regime

When $\epsilon \ll E^{\frac{1}{2}}$, exact solutions can be found. The differential equation for the stream function for linear viscous flow is

$$\nabla^2\psi + J(\psi, h/E^{\frac{1}{2}}) = \tfrac{1}{2}\zeta_T. \tag{5.1}$$

The general technique for finding ψ is first to solve (5.1) using (3.1) and (3.2) with some initial estimate for Q. The transport equation (3.12) can then be used to get a better estimate for Q, and the process is repeated until the solutions converge.

In the special case in which $\mathbf{u}_T$ is irrotational (so that ζ_T is everywhere zero), the system can be solved without iteration by putting

$$\psi = Q\Psi. \tag{5.2}$$

Then Ψ is uniquely determined by

$$\nabla^2\Psi + J(\Psi, h/E^{\frac{1}{2}}) = 0, \tag{5.3a}$$

$$\Psi(r_1, \theta) = 0, \quad \Psi(r_2, \theta) = 1 \tag{5.3b, c}$$

and the transport is found from

$$Q\left[1 + (2\pi E^{\frac{1}{2}})^{-1} \int_{r_1}^{r_2} r^{-1} \int_{-\pi}^{\pi} h_\theta \Psi \, d\theta \, dr\right] = Q_0. \tag{5.4}$$

Analytic solutions of (5.1) satisfying (3.1) and (3.2) with some given estimate for Q can be found when the flow is driven by a rigid lid for the following case. Suppose

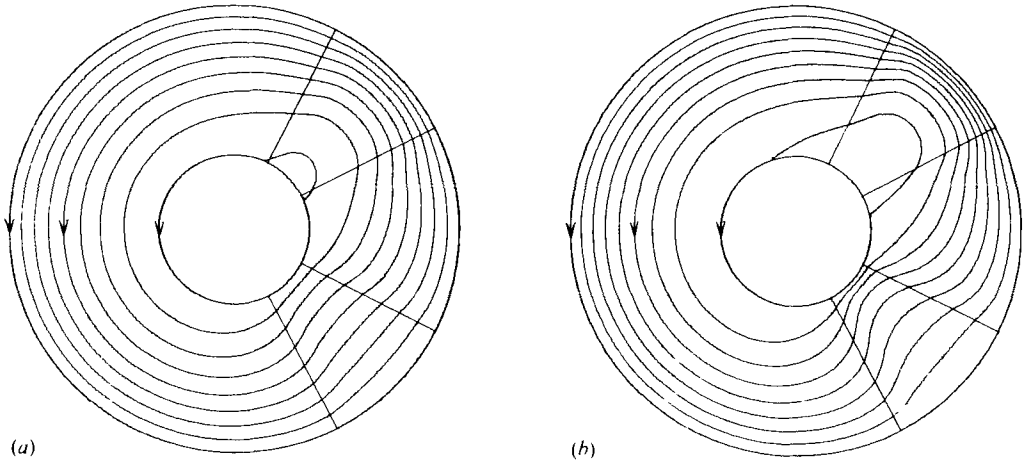

FIGURE 5. Linear viscous flow over plateau topography, stream function contoured at equal intervals. (*a*) $h_0/E^{\frac{1}{2}} = 2$, $Q = 1{\cdot}8$, $\psi_{\min} = -0{\cdot}01$. (*b*) $h_0/E^{\frac{1}{2}} = 4$, $Q = 1{\cdot}5$, $\psi_{\min} = -0{\cdot}08$.

that the bottom topography varies with θ only and is piecewise linear and continuous. Then in a section of constant slope $E^{\frac{1}{2}}S$, the stream-function equation is

$$\nabla^2\psi + \psi_r S/r = \Omega_T. \tag{5.5}$$

The solution is found by separating the variables. This gives a particular solution

$$\psi_P = \begin{cases} \frac{1}{4}\Omega_T r^2 + a_0 + b_0 \ln(r/r_0) & \text{for } S = 0, \\ \Omega_T r^2/(4+2S) + c_0 + d_0(r/r_0)^{-S} & \text{for } S \neq 0, -2, \\ \frac{1}{2}\Omega_T r^2 \ln r + e_0 r^2 + f_0 & \text{for } S = -2 \end{cases} \tag{5.6}$$

and a homogeneous solution

$$\psi_H = (r/r_0)^{-S} \sum_{n=1}^{\infty} (a_n \cosh \beta_n \theta + b_n \sinh \beta_n \theta) \cos[\alpha_n \ln(r/r_0)], \tag{5.7}$$

where $$r_0 = (r_1 r_2)^{\frac{1}{2}}, \quad \alpha_n = (2n-1)\pi/\ln(r_2/r_1), \quad \beta_n^2 = \alpha_n^2 + \tfrac{1}{4}S^2.$$

The constants a_0, b_0, c_0, d_0, e_0 and f_0 are determined from the side-wall conditions. The coefficients a_n and b_n are found by matching the solutions in each section, with the requirement that ψ, ψ_r and ψ_θ be continuous. In practice this involves truncating the series and applying a Galerkin method.

Solutions were calculated for the symmetric plateau topography shown in figure 2. It was found that two or three terms were sufficient to get a good approximation to the solution over most of the annulus and that about five iterations were needed to find Q starting from $Q = Q_0$. However, for the same computational effort, better solutions were obtained numerically by the direct inversion of finite-difference equations. This approach was simplified by first transforming the annulus into a periodic channel.

Numerical solutions are shown in figures 5(*a*) and (*b*) for $\delta = h_0/E^{\frac{1}{2}} = 2$ and $\delta = 4$ respectively. The exact solutions show the same features as the perturbation results. Figures 3(*a*) and 5(*a*) can be compared directly. The gyre is slightly smaller and the transport slightly larger for the exact results. The exact solution is not quite anti-symmetric with respect to θ, and the vorticity is a function of r as well as θ. However, the differences are minor so the perturbation solution is a good approximation for $\delta = 2$.

When δ is doubled, the size of the gyre is increased. The flow within the gyre is still quite weak, being about one-twentieth of the circumpolar transport. A perturbation solution for $h_0/E^{\frac{1}{2}} = 4$ gives a second gyre near the outer side wall. This feature is not seen in the exact result, so the first-order perturbation is no longer a good estimate when $\delta = 4$.

Q decreases monotonically as $h_0/E^{\frac{1}{2}}$ increases, as shown in figure 8. The dependence on δ is initially parabolic, as predicted by the perturbation theory, but becomes linear as δ increases. Comparison with the perturbation estimate (figure 4) shows that Q becomes increasingly larger than the estimated Q as δ increases. An explanation of this behaviour is that the topographic effect $\mathbf{u}.\nabla h$ depends on the speed of the flow. When Q is reduced, as in the first iteration, the average flow speed decreases, so the flow perturbation decreases and the next estimate of Q is larger. For $h_0/E^{\frac{1}{2}} > 6$ the streamline deviations are large, and numerical difficulties were encountered.

The exact stream function is proportional to Ω_T, so the flow pattern depends only on the geometry of the system. This is a consequence of the linear viscous flow being independent of ϵ, and is not true when inertial effects are significant. The stream function is also independent of the average dimensional depth when $\epsilon \ll E^{\frac{1}{2}}$.

6. The inviscid regime

In the inviscid regime, the vorticity equation is

$$\nabla^2\psi + h/\epsilon = F(\psi). \tag{6.1}$$

Using the circulation condition (3.19), an expression for $F(\psi)$ involving ζ_T, $u_I^{(0)}$ and h can be found. From Green's theorem, the integral of the vorticity in the area A of the r, θ plane enclosed by any two streamlines ψ_1 and ψ_2 is

$$\iint_A \zeta \, dA = \Gamma(\psi_1) - \Gamma(\psi_2). \tag{6.2}$$

Hence the circulation condition gives

$$\iint \nabla^2\psi \, dA = \frac{1}{2}\iint \zeta_T \, dA. \tag{6.3}$$

The area element dA is replaced by $U^{-1}ds\,d\psi$, where the arc length s is measured along a streamline and U is the speed of the zeroth-order flow. Since (6.3) is true for any two streamlines, it follows that

$$\oint U^{-1}\nabla^2\psi \, ds = \frac{1}{2}\oint U^{-1}\zeta_T \, ds, \tag{6.4}$$

where the path of integration is a streamline. Substituting for $\nabla^2\psi$ from (6.1) leads to

$$F(\psi) = \oint Wh/\epsilon ds + \frac{1}{2}\oint W\zeta_T \, ds, \tag{6.5}$$

where

$$W(\psi, s) = U^{-1} \Big/ \oint U^{-1} ds$$

acts as a normalized weighting function. (This result can also be obtained from the vorticity equation by including terms to $O(E^{\frac{1}{2}})$.)

An immediate consequence of (6.5) is that a reference level for the topographic stretching of a fluid column following any streamline ψ is

$$h_{\mathrm{ref}}(\psi) = \oint W h \, ds \tag{6.6}$$

(i.e. the topographically generated vorticity is zero where $h = h_{\mathrm{ref}}$). The height of the topography is weighted by the time taken for a fluid column to cross it, the weight favouring regions where the flow is relatively slow. The value of h_{ref} is bounded by the maximum and minimum values of h found along that streamline.

The second integral in (6.5) is similarly a weighted average of the driving vorticity felt by the flow around a streamline. For the special case of an annulus with $\zeta_T = 2\Omega_T$ this term simplifies to

$$\frac{1}{2}\oint W \zeta_T \, ds = \Omega_T,$$

which is independent of ψ. The vorticity equation is then

$$\nabla^2\psi + h/\epsilon = h_{\mathrm{ref}}(\psi)/\epsilon + \Omega_T. \tag{6.7}$$

Solutions of (6.7) subject to the boundary conditions (3.1) and the circulation condition (4.19) have been obtained numerically for a topography $h(\theta)$. The method is iterative. A first estimate of ψ is found by solving

$$\nabla^2\psi + h/\epsilon = \bar{h}/\epsilon + \Omega_T \tag{6.8}$$

such that $$\psi(r_1, \theta) = 0, \quad \psi(r_2, \theta) = Q_0.$$

(This is equivalent to the inviscid limit of the perturbation problem to $O(\delta)$.) An improved estimate ψ_{new} is then found by solving

$$\nabla^2\psi_{\mathrm{new}} + h/\epsilon = h_{\mathrm{ref}}(\psi_{\mathrm{old}})/\epsilon + \Omega_T, \tag{6.9}$$

where ψ_{old} is the previous estimate. The transport Q is corrected at each iteration by applying the circulation condition in the form

$$Q_{\mathrm{new}} = \tfrac{1}{2} Q_{\mathrm{old}} \Gamma_T(\psi_{\mathrm{old}})/\Gamma(\psi_{\mathrm{old}}). \tag{6.10}$$

The rationale for this is as follows. We want to end up with $Q\Gamma(\psi) = \frac{1}{2}Q\Gamma_T(\psi)$. The term $\Gamma_T(\psi)$ is independent of Q while $\Gamma(\psi)$ increases as Q increases. If

$$\Gamma(\psi_{\mathrm{old}}) > \tfrac{1}{2}\Gamma_T(\psi_{\mathrm{old}})$$

then $\Gamma(\psi)$ needs to be reduced (and vice versa), and this is achieved by applying (6.10).

Plateau topography is again used as an example. The choice of a symmetric $h(\theta)$ simplifies the actual calculations because the stream function has the same symmetry. For $h_0/\epsilon\Omega_I = 4$, the streamlines for the original estimate are given in figure 3(*d*) and those of the final solutions are shown in figure 6. Figure 7 shows initial and final streamlines for $h_0/\epsilon\Omega_I = 6$. The initial solutions are modified in the following way. In a gyre near the inner side wall, $h_{\mathrm{ref}} < \bar{h}$ because $h < \bar{h}$ there. In particular $h_{\mathrm{ref}} \to h_{\mathrm{min}}$ as $\psi \to \psi_{\mathrm{min}}$ in such a region. Similarly $h_{\mathrm{ref}} > \bar{h}$ in a gyre near the outer side wall and $h_{\mathrm{ref}} \to h_{\mathrm{max}}$ as $\psi \to \psi_{\mathrm{max}}$. Consequently the vorticity perturbation in a gyre region is decreased in magnitude. In the circumpolar flow region the flow near the inner side wall is relatively slow away from the plateau, and conversely for flow near the outer side wall. Hence $h_{\mathrm{ref}} > \bar{h}$ for streamlines near the inner side wall and h_{ref} increases as

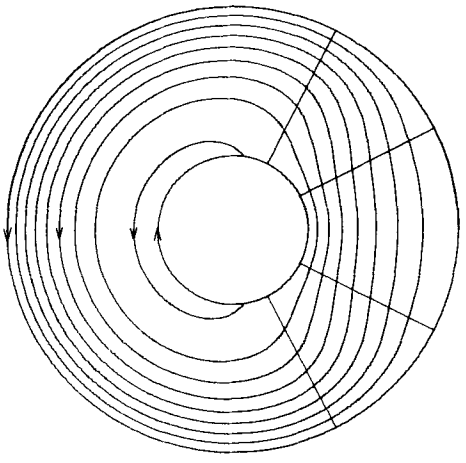

FIGURE 6. Inviscid flow over plateau topography, stream function contoured at equal intervals. $h_0/\epsilon\Omega_I = 4$, $Q = 1{\cdot}65$, $\psi_{\min} = -0{\cdot}01$.

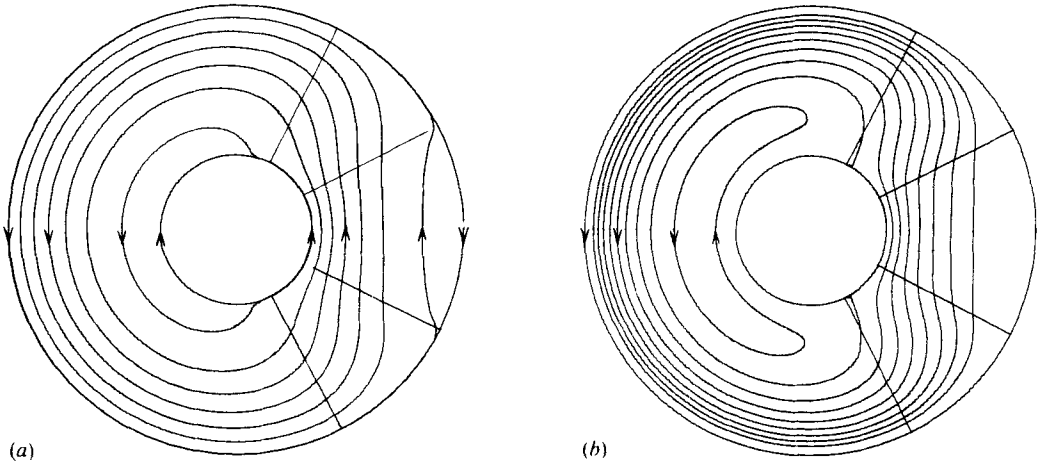

(*a*) (*b*)

FIGURE 7. Inviscid flow over plateau topography, stream function contoured at equal intervals, $h_0/\epsilon\Omega_I = 6$. (*a*) Initial solution. (*b*) Final solution $Q = 1{\cdot}15$, $\psi_{\min} = -0{\cdot}2$.

ψ increases. The overall effect is that where the flow is relatively slow the vorticity perturbation is decreased from the original estimate.

Figures 6 and 7 (*b*) give the situation after fifteen iterations, when the solution has definitely converged. The inner gyre has grown in each case, while the outer gyre in figure 7 (*a*) has vanished. The reason for this behaviour is twofold. First, the decrease in the vorticity perturbation in the gyres decreases the tendency for such regions to form. Second, the decrease in transport and associated general slowing down of the flow change the effect of the driving vorticity. When the topography is flat, Ω_T is just the vorticity required for the streamlines to be circles. When Q decreases and Ω_T is unchanged, this vorticity tends to bend the streamlines inwards. This inhibits outer gyres and enhances inner ones.

In both examples the final value of Q is almost the same as the perturbation estimate. (The perturbation and exact values are 1·64 and 1·65 for $\delta = 4$ and 1·18 and

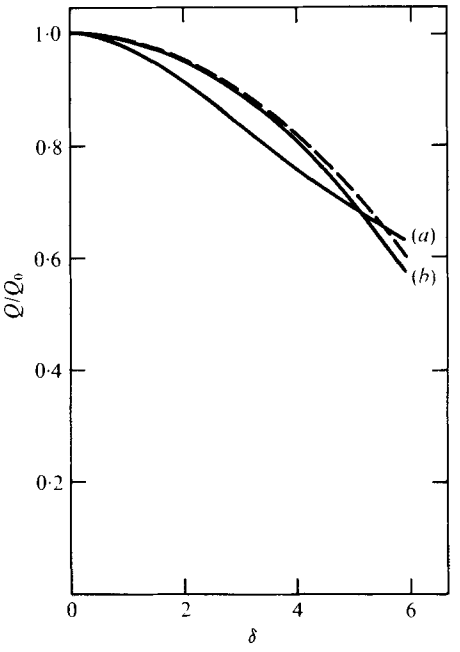

FIGURE 8. Exact transport Q as a function of δ. (a) $\delta = h_0/E^{\frac{1}{2}}$ (linear viscous). (b) $\delta = h_0/\epsilon\Omega_I$ (inviscid). The inviscid perturbation transport to $O(\delta^2)$ is shown as a dashed line for comparison.

1·15 for $\delta = 6$.) For $\delta = 4$ the initial and final flows are very similar, but for $\delta = 6$ there are considerable differences. Hence for the inviscid regime the perturbation solutions are good approximations for δ up to about 4.

The transport Q is plotted against δ in figure 8, and it is seen that Q decreases monotonically as $h_0/\epsilon\Omega_I$ increases. There is close agreement of the exact Q with the perturbation estimate.

It is found that, apart from closed-streamline regions over flat topography, where h_{ref} is constant, $h_{\text{ref}}(\psi)$ increases as ψ increases. Consequently $dF/d\psi \geqslant 0$ for the plateau-topography example. Arnold (1965) has shown that a solution of an equation like (6.1) is stable if $dF/d\psi > 0$ for all ψ so the solution will definitely be stable if there are no gyres. When gyres are present, stability is not guaranteed, but the convergence of the solution method suggests that the solutions are stable. The convergence to a definite solution also suggests that the problem may have a unique solution, but as yet I do not have a proof of this. Note that, for a given stream function ψ, the associated topography h is not unique because any topography $h(\psi)$ can be added to a solution for h.

7. Conclusions

Recycling flow over bottom topography in a rotating system has been studied. According to the ratio of the small parameters ϵ and $E^{\frac{1}{2}}$, the problem was divided into three regimes: linear viscous, intermediate and inviscid. In order to have geostrophic flow over ridges, the non-dimensional topography height was restricted to $O(\max(\epsilon, E^{\frac{1}{2}}))$. The recycling nature of the system meant that upstream conditions were not pre-

scribed. By considering the transport of fluid to $O(E^{\frac{1}{2}})$, a circulation condition was established that is believed to be necessary and sufficient to close the problem.

When the effect of Ekman suction dominates inertial effects ($E^{\frac{1}{2}} \gg \epsilon$) the equations governing the geostrophic flow are linear. The topographic effect at any point is determined by the local slope of h in the direction of flow. Disturbances decay rapidly away from obstacles, and recycling usually has only a small effect on the flow pattern. For the inviscid regime, inertial effects dominate and dissipation has a significant effect only on a large length scale. Such a scale exists in a recycling flow, and viscous effects determine the flow via a circulation condition. In this case, recycling has a strong influence on the flow pattern. The different dynamics of these regimes give contrasting flow patterns over symmetric ridges. The inviscid flow is symmetric, whereas the linear viscous flow disturbance shows strong antisymmetric behaviour. A perturbation analysis of the general problem shows the transition from the linear viscous limit to the inviscid limit as $\epsilon/E^{\frac{1}{2}}$ increases.

The theoretical solutions agree qualitatively with the observations by Maxworthy (1977). He gives results and illustrations for flow over narrow radial ridges whose cross-sections form part of a circle for various values of ϵ and $E^{\frac{1}{2}}$. (Maxworthy uses $\epsilon = \Delta\Omega/2\Omega$, where $\Delta\Omega$ is the dimensional differential rotation of the rigid lid.) The spin-up length $\epsilon/E^{\frac{1}{2}}$ then lies between 0·5 and 8 in nearly all cases (the exception being one example with $\epsilon/E^{\frac{1}{2}} \approx 16$). For $\epsilon < E^{\frac{1}{2}}$, the flow is seen to bend sharply inwards over a rise and outwards over a negative slope, and a gyre forms at the inner side wall, starting over the downstream end of an obstacle. In some cases, the gyre extends around almost to the upstream edge of a ridge, even for $\epsilon < E^{\frac{1}{2}}$. (For $\epsilon < E^{\frac{1}{2}}$ this occurs when δ is numerically large, and linear viscous exact solutions also have this behaviour for large $h_0/E^{\frac{1}{2}}$ and narrow obstacles. The large slopes cause large vorticity fluctuations in a small region and hence large and sharp disturbances to the flow.) As ϵ is increased with $E^{\frac{1}{2}}$ fixed the gyre size decreases, and as $\epsilon/E^{\frac{1}{2}}$ is increased the flow pattern over a ridge changes from strongly antisymmetric to nearly symmetric with respect to θ.

The examples of flow over plateau topography show that such obstacles can cause large disturbances to the flow over them and thus can have a significant effect on the transport in the system. As the plateau height is increased, the circumpolar flow is partially blocked and the transport decreases. The perturbation estimates of the circumpolar transport Q (as $\delta \to 0$) seem to suggest that the linear viscous and inviscid limits represent bounds on Q. But the exact curves for Q_{vis} and Q_{in} *vs.* δ cross at $\delta \approx 5$ (see figure 8), so this hypothesis is probably incorrect. Nevertheless, the exact Q for the intermediate regime is probably well estimated by an average like

$$Q = (EQ_{\text{vis}} + \epsilon^2\Omega_I^2 Q_{\text{in}})/(E + \epsilon^2\Omega_I^2),$$

at least for values of δ not too far in excess of 5.

For the inviscid limit, there is close agreement between the perturbation estimate and the exact Q. (Graphs for both are shown in figure 8.) Hence the perturbation solution is useful for estimating Q even when there are qualitative differences between the exact flow pattern and that to $O(\delta)$. There is also good agreement between the exact and perturbation calculations for the linear viscous limit for $\delta \lesssim 2$. Hence the perturbation method is expected to give good approximations for the difficult intermediate regime for $\delta \lesssim 2$.

A restriction to slowly varying topography was imposed. However solutions (not given here) have also been obtained by this analysis for step-like obstacles. The problem can be regarded as the limit $\theta_2-\theta_1\to 0$, $S\to\infty$ of a plateau with

$$S(\theta_2-\theta_1) = h_0 = \text{constant},$$

S being the slope. In the linear viscous limit a discontinuity occurs in the geostrophic velocity component parallel to the step edge. For the other regimes there is a discontinuity in vorticity but not in velocity.

Other problems not considered in this theory are ageostrophic effects and lateral diffusion of vorticity; the latter would of course smear out the discontinuities just referred to. When the topographic effects are large and the flow is almost blocked, jets form near the side walls and the side-wall layers would become dynamically important in practice. For geophysical applications the β effect should also be included. This can be incorporated as an additional topographic effect.

I wish to express my thanks to Dr H. E. Huppert for suggesting the problem and for his advice during its subsequent development. The support of a Commonwealth Scholarship is gratefully acknowledged.

Appendix A. Uniqueness of stream function for linear viscous flow

The vorticity equation for linear viscous flow in an annulus with prescribed surface vorticity ζ_T is

$$\nabla^2\psi + J(\psi, h/E^{\frac{1}{2}}) = \tfrac{1}{2}\zeta_T, \tag{A 1a}$$

with boundary conditions

$$\psi(r_1,\theta) = 0, \quad \psi(r_2,\theta) = Q. \tag{A 1b, c}$$

Suppose that a function ψ_1 satisfies (A 1) with corresponding transport $Q = Q_1$. Then an infinite set of solutions of (A 1) is given by

$$\psi = \psi_1 + Q_2\Psi, \tag{A 2}$$

where Q_2 is arbitrary and Ψ is the function uniquely determined by (5.3). Hence (A 1) cannot have a unique solution if Q is not specified.

The reason for this non-uniqueness is that insufficient information about the surface velocity $\mathbf{u}_T$ has been included in the mathematical description. There are infinitely many velocity distributions $\mathbf{u}_T$ with the same vorticity distribution ζ_T. The problem is that Q depends upon $\mathbf{u}_T$ as well as ζ_T. The extra condition

$$Q = Q_0 - (2\pi E^{\frac{1}{2}})^{-1}\int_{r_1}^{r_2} r^{-1}\int_{-\pi}^{\pi} h_\theta\psi\, d\theta\, dr, \tag{A 3}$$

where

$$Q_0 = \frac{1}{2}\int_{r_1}^{r_2} v_T\, dr,$$

is sufficient to resolve the problem. Suppose that two functions ψ_1 and ψ_2 satisfy (A 1) and (A 3), with transports Q_1 and Q_2 respectively. Then it is found that

$$\psi_1 - \psi_2 = (Q_1 - Q_2)\Psi \tag{A 4}$$

and

$$Q_1 - Q_2 = -(Q_1 - Q_2)(2\pi E^{\frac{1}{2}})^{-1}\int_{r_1}^{r_2} r^{-1}\int_{-\pi}^{\pi} h_\theta\Psi\, d\theta\, dr. \tag{A 5}$$

Hence $Q_1 = Q_2$ unless

$$-(2\pi E^{\frac{1}{2}})^{-1}\int_{r_1}^{r_2} r^{-1}\int_{-\pi}^{\pi} h_\theta \Psi\, d\theta\, dr = 1. \tag{A 6}$$

Equations (5.3) can be regarded as governing flow in a channel driven by a uniform surface velocity. By methods similar to those in appendix B, it is found that the transport must decrease if the topography is not flat, so the left-hand side of (A 6) must be negative. Hence $\psi_1 = \psi_2$ and the solution of (A 1) with (A 3) is unique.

Appendix B. Transport in an annulus driven by a rigid lid

We define parameters

$$\tau = \oint U^{-1} ds \quad (U \neq 0), \quad l = \oint ds,$$

where the integrals are taken around a streamline for the interior flow. τ is the time taken for a fluid element to complete a circuit of a streamline of length l. By Schwarz's inequality we have

$$\left[\int U^{-\frac{1}{2}} U^{\frac{1}{2}}\, ds\right]^2 = \left(\oint ds\right)^2 \leqslant \int U^{-1} ds \int U\, ds. \tag{B 1}$$

Hence

$$l^2 \leqslant \tau\Gamma,$$

where

$$\Gamma = \int U\, ds \tag{B 2}$$

is the circulation.

For flow in an annulus driven by a rigid lid with $\zeta_T = 2\Omega_T$, the interior velocity is

$$(u_I, v_I) = (0, \tfrac{1}{2}\Omega_T r)$$

when the bottom topography is flat. Then

$$\tau_{I0} = 4\pi/\Omega_T = l^2/\Gamma_{I0} \tag{B 3}$$

(the subscript 0 denotes flat-bottom variables). Consider an irreducible streamline $r = r(\theta)$. By the circulation condition,

$$l^2/\Gamma_I = 2l^2/\Gamma_T = l^2/\Omega_T A, \tag{B 4}$$

where

$$A = \int_{-\pi}^{\pi} \tfrac{1}{2} r^2 d\theta$$

is the area enclosed by $r(\theta)$. Since l is the length of the perimeter of A, we have

$$l^2/A \geqslant 4\pi, \tag{B 5}$$

with equality if and only if A is circular. Hence

$$l^2/\Gamma_I \geqslant 4\pi/\Omega_T.$$

Then, by (B 2) and (B 3),

$$\tau_I \geqslant \tau_{I0}. \tag{B 6}$$

Thus any fluid element takes longer to travel around the annular region when the streamlines are not circular. Hence any azimuthal variation in the topography must cause a decrease in the net transport Q. (The streamlines remain circular for topography which is a function of r alone.)

REFERENCES

ARNOLD, V. I. 1965 Conditions for nonlinear stability of stationary plane curvilinear flows of an ideal fluid. *Dokl. Acad. Sci. USSR* **162**, 773–777.

BATCHELOR, G. K. 1956 On steady laminar flow with closed streamlines at large Reynolds number. *J. Fluid Mech.* **1**, 177–190.

BOYER, D. L. 1971*a* Rotating flow over long shallow ridges. *Geophys. Fluid Dyn.* **2**, 165–184.

BOYER, D. L. 1971*b* Rotating flow over a step. *J. Fluid Mech.* **50**, 675–687.

CARRIER, G. F. 1965 Some effects of stratification and geometry in rotating fluids. *J. Fluid Mech.* **23**, 145–172.

GILL, A. E. & PARKER, R. L. 1970 Contours of 'h cosec θ' for the world's oceans. *Deep-Sea Res.* **17**, 823–824.

HART, J. E. 1977 A note on quasi-geostrophic flow over topography in a bounded basin. *J. Fluid Mech.* **79**, 657–668.

HUPPERT, H. E. & STERN, M. E. 1974*a* Ageostrophic effects in rotating stratified flow. *J. Fluid Mech.* **62**, 369–385.

HUPPERT, H. E. & STERN, M. E. 1974*b* The effect of side walls on homogeneous rotating flow over two-dimensional obstacles. *J. Fluid Mech.* **62**, 417–436.

JOHNSON, J. A. & HILL, R. B. 1975 A three-dimensional model of the Southern Ocean with bottom topography. *Deep-Sea Res.* **22**, 745–752.

KAMENKOVICH, V. M. 1962 On the theory of the Antarctic Circumpolar Current. *Akad. Nauk SSR Inst. Okean. Trudy* **56**, 241–293.

MAXWORTHY, T. 1977 Topographic effects in rapidly rotating fluids: flow over a transverse ridge. *Z. angew. Math. Phys.* **28**, 853–864.

STEWARTSON, K. 1957 On almost rigid rotations. *J. Fluid Mech.* **3**, 17–26.